Vaccine 40 (2022) 4872–4880

Contents lists available at ScienceDirect

Vaccine

journal homepage: www.elsevier.com/locate/vaccine

Streptococcus pneumoniae serotype 15B polysaccharide conjugate elicits a cross-functional immune response against serotype 15C but not 15A

Li Hao [a], Michelle M. Kuttel [b], Neil Ravenscroft [c], Allison Thompson [a], A. Krishna Prasad [a,1], Seema Gangolli [a], Charles Tan [a], David Cooper [a], Wendy Watson [d], Paul Liberator [a], Michael W. Pride [a], Kathrin U. Jansen [a], Annaliesa S. Anderson [a], Ingrid L. Scully [a,*]

[a] *Pfizer Vaccine Research & Development, 401 N. Middletown Rd, Pearl River, NY 10965, USA*
[b] *Department of Computer Science, University of Cape Town, Rondebosch 7701, South Africa*
[c] *Department of Chemistry, University of Cape Town, Rondebosch 7701, South Africa*
[d] *Pfizer Vaccine Clinical Research & Development, 500 Arcola Rd, Collegeville, PA 19422, USA*

ARTICLE INFO

Article history:
Received 2 March 2022
Received in revised form 9 June 2022
Accepted 13 June 2022
Available online 7 July 2022

Keywords:
Streptococcus pneumoniae
Serogroup 15
Polysaccharide conjugate vaccine
PCV20
Opsonophagocytic activity

ABSTRACT

Protection conferred by pneumococcal polysaccharide conjugate vaccines (PCVs) is associated with PCV-induced antibodies against vaccine-covered serotypes that exhibit functional opsonophagocytic activity (OPA). Structural similarity between capsular polysaccharides of closely related serotypes may result in induction of cross-reactive antibodies with or without a cross-functional activity against a serotype not covered by a PCV, with the former providing an additional protective clinical benefit. Serotypes 15B, 15A, and 15C, in the serogroup 15, are among the most prevalent *Streptococcus pneumoniae* serotypes associated with invasive pneumococcal disease following the implementation of a 13-valent PCV; in addition, 15B contributes significantly to acute otitis media. Serological discrimination between closely related serotypes such as 15B and 15C is complicated; here, we implemented an algorithm to quickly differentiate 15B from its closely related serotypes 15C and 15A directly from whole-genome sequencing data. In addition, molecular dynamics simulations of serotypes 15A, 15B, and 15C polysaccharides demonstrated that while 15B and 15C polysaccharides assume rigid branched conformation, 15A polysaccharide assumes a flexible linear conformation. A serotype 15B conjugate, included in a 20-valent PCV (PCV20), induced cross-functional OPA serum antibody responses against the structurally similar serotype 15C but not against serotype 15A, both not included in PCV20. In PCV20-vaccinated adults (18–49 years), robust OPA antibody titers were detected against both serotypes 15B (the geometric mean titer [GMT] of 19,334) and 15C (GMTs of 1692 and 2747 for strains PFE344340 and PFE1160, respectively), but were negligible against serotype 15A (GMTs of 10 and 30 for strains PFE593551 and PFE647449, respectively). Cross-functional 15B/C responses were also confirmed using sera from a larger group of older adults (60–64 years).

1. Introduction

Streptococcus pneumoniae, a Gram-positive facultative anaerobe, is a common colonizer of the human respiratory tract and causes invasive pneumococcal disease in adults and children and also contributes significantly to acute otitis media in children (https://www.cdc.gov/vaccines/pubs/pinkbook/downloads/pneumo.pdf). Children younger than 5 years and elderly are the most vulnerable populations affected by *S. pneumoniae* (https://www.cdc.gov/pneumococcal/index.html) [1–4].

S. pneumoniae expresses a polysaccharide capsule which is an important virulence factor and vaccine target [5–7]. Pneumococcal serotypes are classified based on the chemical structure of capsular polysaccharides, with the capsule diversity caused by variation in oligosaccharide units or attached side groups. Structurally related polysaccharide serotypes form pneumococcal serogroups [7,8]. Genetically encoded by the capsular polysaccharide biosynthesis (*cps*) locus, nearly 100 serotypes have been identified to date [9].

Pneumococcal polysaccharide conjugate vaccines (PCVs) elicit serotype-specific protective antibodies that exhibit opsonophagocytic activity (OPA), e.g., facilitate complement-mediated uptake

* Corresponding author.
E-mail address: Ingrid.Scully@pfizer.com (I.L. Scully).
[1] Permanent address: Citranvi Biosciences, LLC, Chapel Hill, NC 27516.

https://doi.org/10.1016/j.vaccine.2022.06.041
0264-410X/

and killing of the pneumococcus by human phagocytic effector cells such as neutrophils [10–14]. Some closely related serotypes can generate cross-reactive anti-capsular antibodies that may or may not also confer cross-functional OPA activity. Evidence of cross-functional antibodies was seen following immunization of infants with a 13-valent PCV (PCV13), resulting in development of serum antibodies with OPA activity against serotypes 6C and 7A that were not included in the vaccine [15]. New serotypes included in the 20-valent PCV (PCV20), approved by the U.S. FDA for adults ages 18 years or older [16], may also elicit cross-functional antibodies against serotypes expressing structurally similar polysaccharides, such as serotype 15B.

Capsular polysaccharides of serotypes 15A, 15B, and 15C are closely related, with 15A having a linear repeat unit structure, while 15B and 15C have a branched repeat unit structure [17,18] (Fig. 1). Serotypes 15B and 15C share almost identical genetic sequence across the *cps* operon, except for a variation in the number of thymine-adenine (TA) tandem repeats near the 5′ end of *wciZ* [19,20]. *WciZ*, encoding a membrane-bound *O*-acetyltransferase, is known to be functional in 15B but not in 15C due to an out-of-frame mutation associated with the TA repeat units [21]. Distinguishing 15B and 15C isolates from one another using serological methods is complicated given the closely related structure; consequently, serogroup 15 isolates are often reported as 15B/C in the PubMLST database (https://pubmlst.org/spneumoniae/) and other publications [22–24].

Here, we describe an algorithm to quickly differentiate 15B from its closely related serotypes 15C and 15A directly from whole-genome sequencing (WGS) data. A serotype 15B capsular polysaccharide conjugate, included in PCV20, was also investigated for the ability to induce cross-functional antibody responses to serotypes 15A and 15C (not contained in PCV20) in human sera collected from adults vaccinated with PCV20. Computer modeling of the serotype 15A/B/C oligosaccharide chain structure, based on the measure of conformational extension and flexibility of polysaccharide repeat units, the end-to-end distance [25], provides further insight into the molecular basis of potential cross-protection among serotypes in pneumococcal serogroup 15.

2. Materials and methods

2.1. S. pneumoniae strains used for validation of in silico 15A/B/C serotyping approach

The PubMLST Pneumococcal Genome Library (PGL) is a collection of > 9,000 published genomes hosted within the PubMLST *S. pneumoniae* database (https://pubmlst.org/spneumoniae/pgl). As of 09/16/2020, there are 365 serotype 15A strains and 416 serotype 15B, 15C, or 15B/C strains. Furthermore, a total of 7,770 *S. pneumoniae* strains were identified from PGL assigned to a serotype other than serogroup 15. WGS data of these strains were used to test the specificity and sensitivity of a 15A nucleotide sequence marker and to better understand the genetic polymorphism between serotypes 15B and 15C.

2.2. Molecular modeling of 15A, 15B and 15C polysaccharide conformations

2.2.1. Molecular dynamics

Simulations were performed with version 2.12 of the Nanoscale Molecular Dynamics (NAMD) program [26], using CUDA extensions for calculation of long-range electrostatic forces and non-bonded forces on graphics processing units [27]. The carbohydrates were modeled with the CHARMM36 additive force field for carbohydrates [28,29], incorporating ad hoc extensions to represent the phosphodiester linkages. The torsion angles describing the confor-

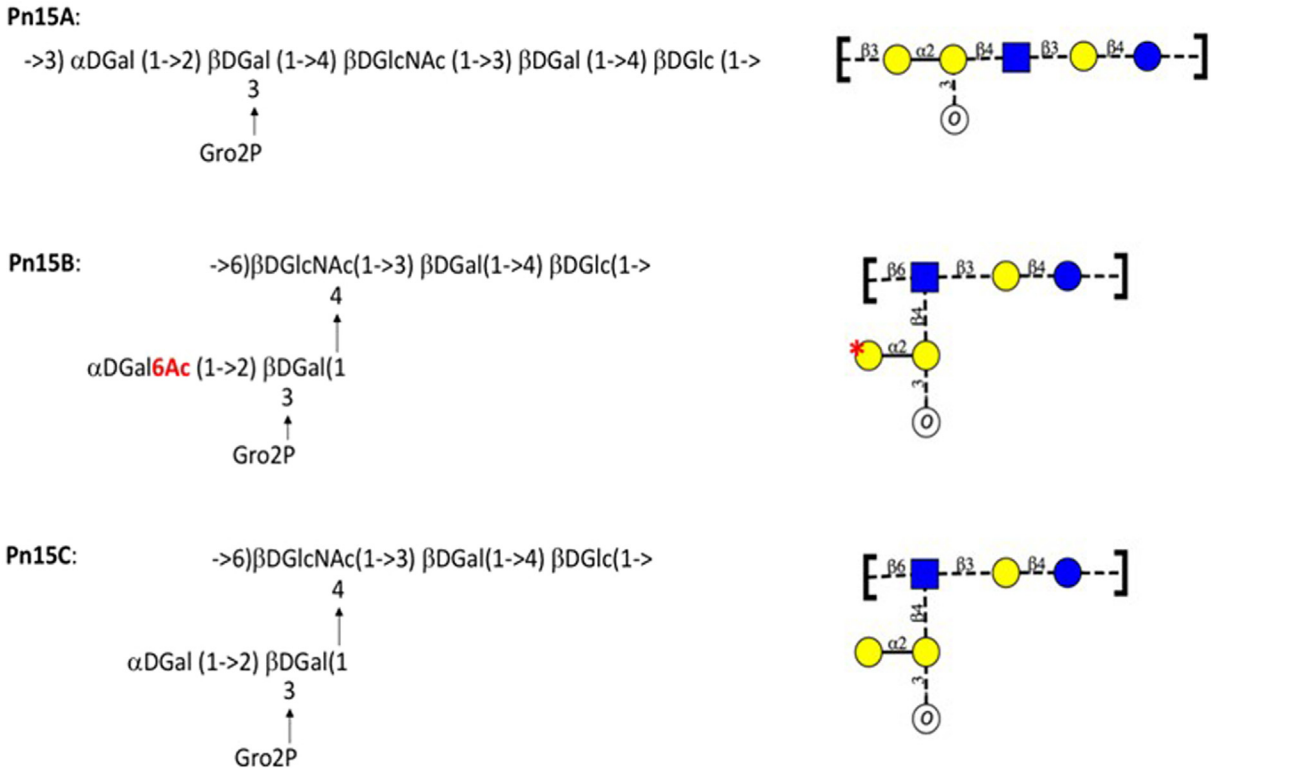

Fig. 1. *S. pneumoniae* serotype 15A, 15B, and 15C polysaccharide structures. The position of *O*-acetylation of the serotype 15B polysaccharide side chain is highlighted (*and 6Ac). Residues are colored according to type: blue – Glc/GlcNAc, yellow – Gal, white – Gro2P (glycerol-phosphate). Pn15A, Pn15B and Pn15C, *S. pneumoniae* serotypes 15A, 15B and 15C, respectively.

mation of the linkages are here defined as: φ = H1-C1-O1-CX'; ψ = C1-O1-CX'-OX'. Water was simulated with the TIP3P water model [30], which is compatible with the CHARMM36 carbohydrate force field.

The initial structures for the 3 repeat units (3RU) simulations were built using our CarbBuilder software [31]. All initial structures were subjected to 10,000 steps of standard NAMD minimization in vacuum, followed by solvation in a cubic water box using the Visual Molecular Dynamics (VMD) software [32]. Sodium ions were randomly distributed in each simulation using VMD, to neutralize the negative charge from each phosphodiester.

All MD simulations began with a 122,000-step minimization-and-heating phase which consisted of 5 K temperature reassignments from an initial 10 K up to a temperature of 310 K, with 1,000 steps of minimization and 1,000 steps of MD at each temperature. Simulations of each 3RU chain were run for 250 ns, with the first 50 ns discarded as equilibration in the subsequent data analysis.

The MD equations of motion were integrated with a Leap-Frog Verlet integrator with a step size of 1 fs and periodic boundary conditions were employed. Simulations were run under the isothermal-isobaric (nPT) ensemble at 310 K, which was sustained by a Langevin piston barostat and a Nose-Hoover thermostat (a combination of the Nose-Hoover constant pressure method [33] with piston fluctuation control implemented using Langevin dynamics [34] as implemented in NAMD [26]). Long range electrostatics were calculated with particle mesh Ewald (PME) [35] summation using k = 0.20 Å-1 and PME grid dimensions were set to be equal to the periodic cell dimensions of the system. Non-bonded interactions were truncated at 15.0 Å with a switching function employed between 12.0 and 15.0 Å. The 1–4 interactions were not scaled, in accordance with CHARMM force field recommendations.

2.2.2. Data analysis

For each simulation, molecular conformations were extracted at 25 ps intervals. The first 50 ns of each simulation was discarded as equilibration, to allow for the flexible polysaccharides to relax from their initial conformations.

Inter-atomic distances and dihedral angles were extracted using VMD's Tcl scripting interface. Statistical values were calculated with in-house Python scripts and graphs. Molecular conformations extracted from the MD simulations were depicted with VMD.

The most common chain conformations are determined by clustering the simulation conformations into families. Before conformational clustering, all the simulation conformations were aligned on the ring atoms of the GlcNAc residue in the central repeat unit of the 3RU chain. VMD's internal cluster command with a cut-off of 5.0 Å was used to calculate the clusters with a Root Mean Square Deviation (RMSD) fit to the non-hydrogen atoms in residues 3 to 15 in the chain (the terminal residues are more flexible and hence less representative of the conformation of the native O-Ag polysaccharide). Clusters comprising less than 5% of the simulation were excluded from analysis.

2.3. Evaluation of cross-functional human serum OPA against S. pneumoniae serogroup 15 serotypes

2.3.1. Selection of S. pneumoniae strains

Two 15A (PFE593551 and PFE647449) and two 15C (PFE344340 and PFE1160) strains of *S. pneumoniae* serotypes were selected, in addition to the clinical 15B strain PFESP05051.

2.3.2. Human sera

Residual sera used for exploratory analysis of cross-functional responses among *S. pneumoniae* serotypes 15A, 15B, and 15C were from pneumococcal vaccine-naïve healthy adults 18 to 49 years of age who were administered a single dose of either PCV20 (which contains serotype 15B capsular polysaccharide conjugate) or the licensed tetanus, diphtheria, acellular pertussis combination vaccine (Tdap; control) (B7471001; NCT02955160). For confirmation, residual sera were obtained from larger groups of adults, 60 to 64 years of age, who were vaccinated with a single dose of either PCV20 or PCV13 (does not contain serotype 15B capsular polysaccharide conjugate; control) for exploratory analysis (B7471002; NCT03313037). Sera were collected one month after the vaccine dose.

2.3.3. OPA assays

OPA assays have been described previously [10,12,15,36]. Here, OPA assays were developed for pneumococcal serotypes 15A, 15B, and 15C. Briefly, heat-inactivated sera were serially diluted 2.5-fold in Hanks' balanced saline solution supplemented with 0.1% gelatin. Target bacteria were added to assay plates and were incubated for 30 min at 37○C on a shaker. Baby rabbit complement (3- to 4-week–old, Pel-Freez, 6% final concentration) and differentiated HL-60 cells were then added to each well at an approximate effector to target ratio of 200:1. Assay plates were incubated for 45 min at 37○C, 5% CO_2 at shaking. A 10-μL aliquot of the incubated mixture was transferred to the wells of Millipore, MultiScreenHTS HV filter plates containing 50 μL of 2% HL-60 lysate in distilled water. Liquid was filtered through the plates under vacuum, and 50 μL of HySoy medium was added to each well and filtered through. The filter plates were then incubated at 37○C, 5% CO_2 overnight and the resulting colonies were then stained with Coomassie Brilliant Blue stain. Colonies were imaged and enumerated on a Cellular Technology Limited (CTL) ImmunoSpot Analyzer®. The OPA antibody titer was interpolated from the reciprocal of the two serum dilutions encompassing the point of 50% reduction in the number of bacterial colonies when compared to the control wells that did not contain immune serum.

Geometric mean titers (GMTs) and correlation coefficients were determined along with 95% confidence intervals (CI) of the correlation of 15C and 15A OPA titers with respect to 15B OPA titers to ascertain the extent of cross-functionality among the serogroup 15 serotypes. A geometric mean ratio (GMR) was also calculated to compare the groups vaccinated with PCV20 and PCV13.

3. Results

3.1. Analysis of genetic relatedness among 15A, 15B, and 15C strains of S. pneumoniae

The polysaccharide structures for serotypes 15A, 15B, and 15C contain a pentasaccharide repeat unit including a glycerol-phosphate residue [17,18]. Serotypes 15B and 15C differ from each other only by the presence (15B) or absence (15C) of the *O*-acetyl group on the αDGal unit in the three-residue side chain [17,37]. In contrast to 15B and 15C, the 15A polysaccharide lacks an oligosaccharide side chain and has a longer backbone repeat unit [18]. The structure of repeat units of the capsular polysaccharides for serotypes 15A, 15B, and 15C is shown in Fig. 1.

3.1.1. In silico approach to differentiate between serotypes 15A and 15B from WGS data

The considerable similarity of the genetic organization of *S. pneumoniae cps* operon of serotypes 15A, 15B and 15C has been previously reported [19]. One of exceptions maps to *wzd*. Over

the final 300 bp of *wzd*, serotype 15A shares only 69% nucleotide sequence identity with 15B and 15C. A 141 bp fragment at the 3′ end of *wzd* from the 15A reference strain 389/39 was selected as a sequence marker diagnostic for serotype 15A. Isolates whose nucleotide sequence matches this fragment when running BLAST in BIGSdb [38] are identified as serotype 15A, whereas a BLAST search of 15B or 15C isolate genome sequences will yield a 111 bp fragment hit with 30 nucleotide differences. Validation of the 141 bp fragment as a diagnostic marker for serotype 15A was then performed by BLAST analysis of a large collection of *S. pneumoniae* genomes from PGL with pre-identified serotypes, including (i) 365 serotype 15A isolates; (ii) 416 serotype 15B, 15C, or 15B/C isolates; and (iii) $\geq$ 7770 non-serogroup 15 isolates from PGL at PubMLST (BLAST output is included in **Supplementary Tables 1 and 2**). Among the 365 pre-identified 15A isolates, 359 have sequence identical to the query fragment. Four isolates differ from the 141 bp diagnostic marker fragment by just 1 to 4 nucleotides. They were typed as 15A by an in-house K-mer–based WGS serotyping algorithm (Lee J. et al, manuscript in preparation). The same algorithm predicted the remaining 2 isolates as 15C and 6A. In contrast to the full-length match to the majority of isolates pre-identified as serotype 15A, none of the 416 15B, 15C, or 15B/C isolates had a full-length BLAST match to the 141 bp marker sequence, except two isolates which were later identified as non-serogroup 15. Similarly, none of the > 7760 non-serogroup 15 isolates from PGL yielded any hits with a perfect match (**Supplementary Table 2**).

3.1.2. Genetic differentiation between serotypes 15B and 15C using TA dinucleotide repeats within wciZ from WGS data

The sequence polymorphism at the *wciZ* TA dinucleotide repeat regions is shown in Fig. 2**A**. To effectively capture the difference of TA repeats and link the number of repeats to the functionality of *wciZ*, a coding system (2TN) was designed (Fig. 2**A**). For example, in 2T9, the first number "2″ represents two TA repeats before nucleotide **T**, and the last number "9" represents the number of TA repeats after nucleotide **T**. An isolate that is typed as 2T9 will yield a premature stop codon and a prediction of serotype 15C, similar to 2T6, 2T7, 2T10, etc. Serogroup 15 strains typed as 2T8 or 2T11 retain an intact open reading frame for *wciZ* and are serotype 15B (Fig. 2**B**).

To better understand the polymorphism of the TA dinucleotide repeats, the full-length sequence of *wciZ* from 400 15B, 15C, or 15B/C isolates were retrieved from PGL and aligned. Using the 2TN coding system, the TA repeat pattern can be inferred for each isolate. Excluding rare ambiguous cases, 6 different TA repeat patterns were observed (Table 1). The most prevalent TA repeat pattern is 2T8, followed by 2T9 and 2T7 (with premature stop codon). Consistent with the polysaccharide structure, the majority of isolates pre-identified as serotype 15B have the TA dinucleotide repeat pattern 2T8 and are predicted to code for a full-length WciZ O-acetyltransferase. Together, strains typed as 2T8 and 2T11 are representative of 90.9% of the isolates pre-identified as serotype 15B, whereas fewer pre-labeled 15C isolates have 2T8 compared to other TA repeats. Given that using serological methods to differentiate 15B and 15C is complicated [39,40], it is possible that those pre-labeled 15C isolates which have the 2T8 repeat pattern are actually 15B, either through mislabeling or interconversion. Among 176 pre-labeled 15B/C isolates, ~52% have 2T8 with intact WciZ, suggesting that they are very likely to be 15B, whereas the remaining 15B/C could be 15C.

3.1.3. Genotypic identification of S. pneumoniae serotype 15C bacterial banks used in OPA

The WGS of 7 isolates pre-identified as serotype 15A, 15B, and 15C was generated and their serotypes were inferred using the TA dinucleotide repeat algorithm. *In silico* serotyping results are shown in Table 2.

3.2. Molecular modeling of 15A/B/C polysaccharide conformation

Molecular dynamics simulations of 3RU of the serotype 15A, 15B, and 15C polysaccharides were performed to compare the flexibility and conformations of the pneumococcal serogroup 15 antigens.

3.2.1. Flexibility

To assess chain flexibility, the end-to-end distance, *r*, was used as a simple measure of conformational extension of the 3RU oligosaccharides. Specifically, *r* was here defined for all antigens as the distance from C1 of the first β-D-GlcNAc residue to C4 of the third β-D-GlcNAc residue (counting from the reducing end) on the polysaccharide backbone.

Comparison of the *r* time series for 15A (Fig. 3**A**) with 15B (Fig. 3**B**) and 15C (Fig. 3**C**) shows a large difference in flexibility. Serotype 15A displays rapid transitions between a broad range of values of *r*, from 6 Å to 45 Å (Fig. 3**A**), with a mean of 32.6 Å (standard deviation 8.4 Å). The corresponding histogram of *r* (Fig. 3**D**)

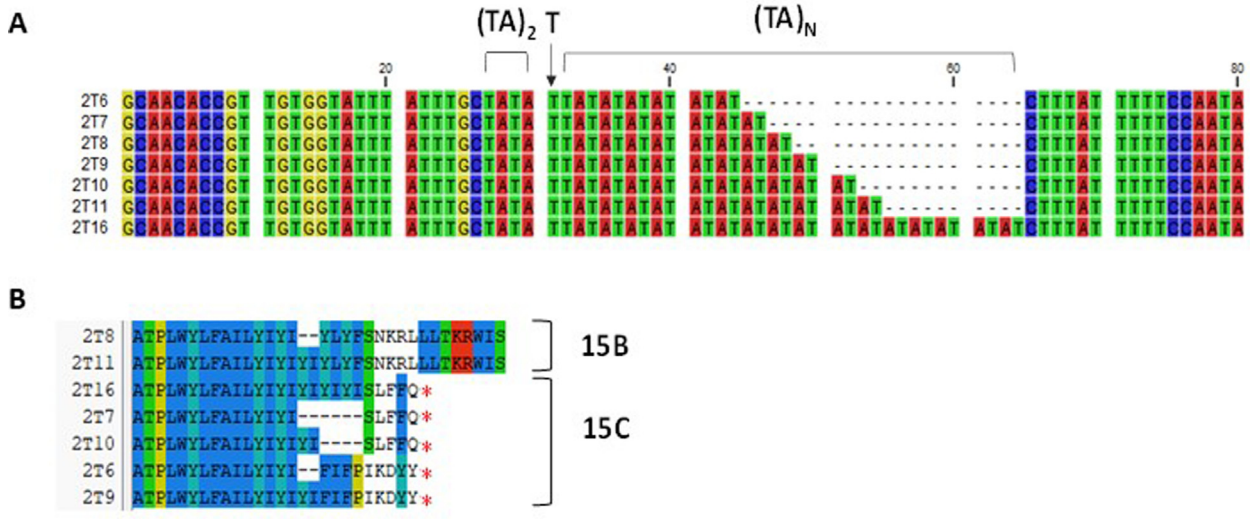

Fig. 2. Alignment of *wciZ* TA repeats and coding system.

Table 1
Distribution of *wciZ* TA dinucleotide repeat patterns from PGL15B, 15C, or 15B/C isolates. The 2T8 and 2T11 repeat patterns result in an intact open-reading frame of *wciZ*, whereas the others introduce a premature stop codon.

Serotype	2T6	2T7	2T8	2T9	2T10	2T11
15B	0	5	68	2	0	2
15C	4	29	58	41	4	0
15B/C	6	36	92	38	4	0

Table 2
WGS results of serogroup 15 isolates. WGS, whole-genome sequencing.

Pre-identified serotype	Strain ID	Whole-genome sequence		
		141 bp *wzd* marker	TA dinucleotide repeat	WGS-predicted serotype
15B	15B-PFESP05051	no	2T8	15B
15C	15C-PFE344340	no	2T9	15C
	15C-PFE1159	no	2T7	15C
	15C-PFE1160	no	2T7	15C
15A	15A-647449	yes	n/a	15A
	15A-593551	yes	n/a	15A
	15A-308551	yes	n/a	15A

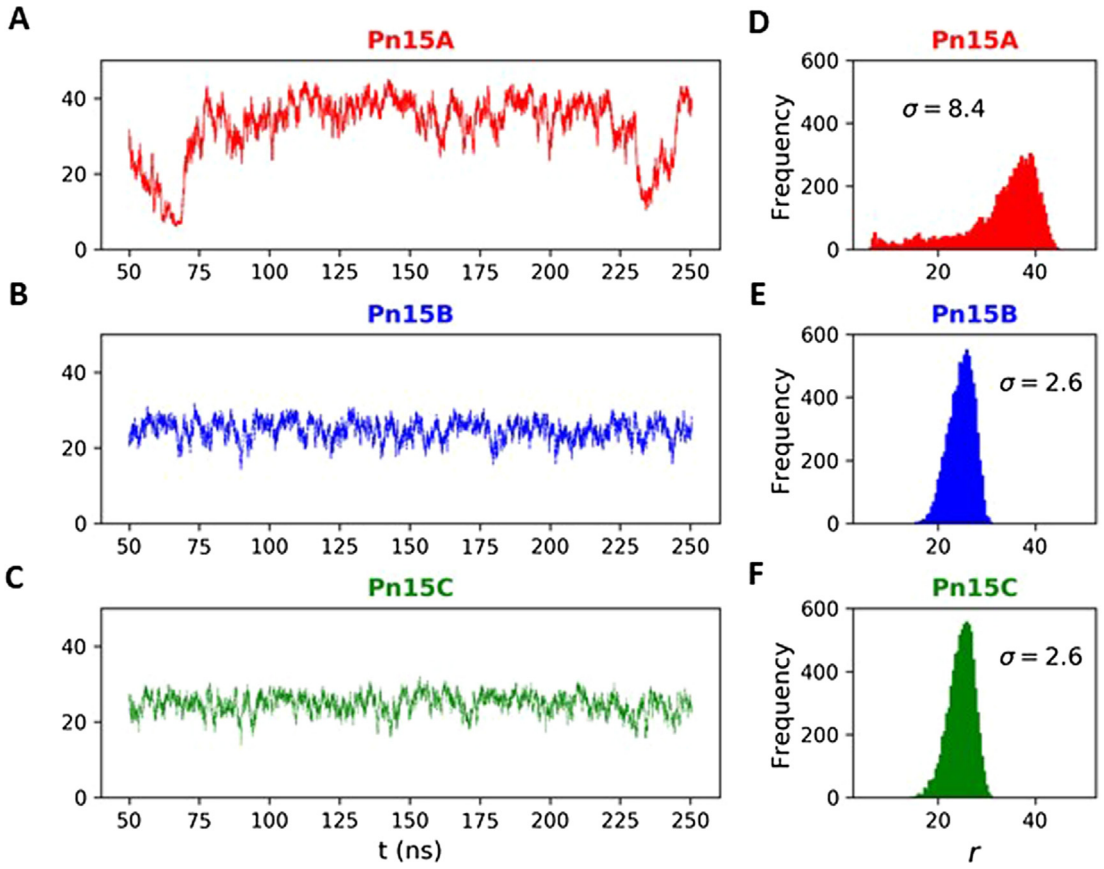

Fig. 3. Comparison of the end-to-end distance, *r*, time series for (**A**) serotype 15A, (**B**) serotype 15B, and (**C**) serotype 15C, excluding the first 50 ns of simulation time. The corresponding histograms of the distance *r* are shown in (**D**), (**E**), and (**F**), respectively. Distances are in Å. Pn15A, Pn15B and Pn15C, *S. pneumoniae* serotypes 15A, 15B, and 15C, respectively.

reflects this broad distribution, which is skewed towards more extended conformations.

In contrast, serotypes 15B and 15C show a much narrower range of *r*, from 14 Å to 32 Å, with identical average values of 24.7 Å (standard deviation 2.6 Å). The corresponding histograms of *r* (Fig. 3**E and F**) show relatively narrow Gaussian distributions for both, indicating that the addition of O-acetylation in 15B does not affect the conformation and dynamics of these oligosaccharides.

3.2.2. Chain conformations

To explore the causes of the observed significant difference in the polysaccharide flexibility of serotypes 15A, 15B, and 15C, the simulation conformations were clustered into families. Serotype

15A has a set of five conformational families, which are shown (with associated populations) in Fig. 4**A**. The 3RU model of 15A polysaccharide molecule is highly mobile and interchanges frequently between these different conformations during the simulation. On a finer scale, the glycerol residue is also very mobile; therefore, the Gro2P(O->3)bDGal group is not likely to present a stationary target for antibody binding. In contrast, 15B and 15C molecules both have a predominant (88%) well-defined "zig-zag" conformation (Fig. 4**B and C**) that is largely maintained throughout the course of the simulation, demonstrating that, compared to 15A, 15B and 15C are much less flexible molecules and have a common structure. To illustrate this conformation on a longer chain, static 12RU models of 15B and 15C polysaccharides were built based on the most populated glycosidic linkage conformations obtained from the 3RU simulations (Fig. 5). This larger model shows that O-acetylation does not alter the zig-zag conformation of the common backbone, but also illustrates how exposed the O-acetyl and glycerol groups are for possible antibody binding.

3.3. Assessment of cross-functional human serum OPA among S. pneumoniae serotypes 15A, 15B, and 15C

To examine if *S. pneumoniae* serotype 15B polysaccharide conjugate included in PCV20 elicits cross-functional responses against related serotypes 15A and 15C in humans, sera from 18 to 49-year–old subjects immunized with a single dose of PCV20 were tested for functional activity against strains serotyped as 15A and 15C using the OPA assay. Analysis of OPA in the PCV20 immune sera (n = 32) demonstrated high antibody titers against serotype 15B (GMT of 19,334), as well as robust titers against both serotype 15C strains (PFE344340 and PFE1160) included in the study, yielding GMTs of 1692 and 2747, and with a correlation to 15B titers of 0.48 and 0.59, respectively. In contrast, the Tdap-immunized negative controls (n = 33) yielded serum GMTs of 34 against serotypes 15B and 9 and 12 against the two serotype 15C strains (Table 3). These data indicate that immunization with the 15B-containing PCV20 is able to elicit cross-functional antibodies that kill serotype 15C isolates.

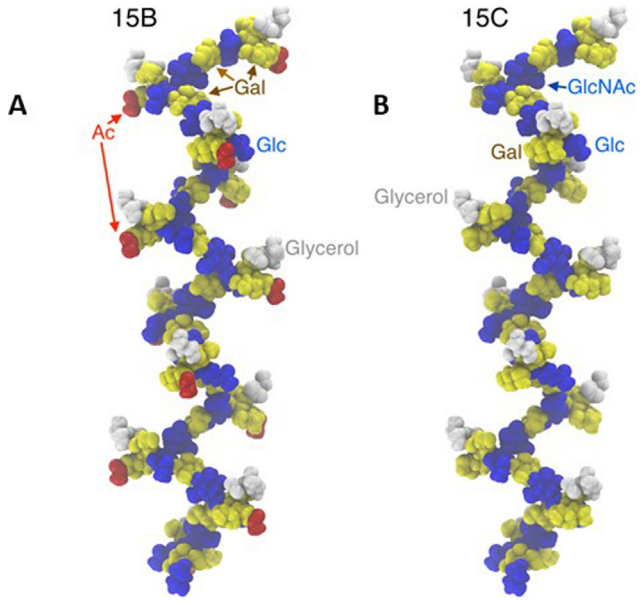

Fig. 5. 12RU static models of 15B (**A**) and 15C (**B**) polysaccharides built with the most populated dihedral angle conformations obtained from the 3RU simulations. The polymers have a common "zig-zag" backbone conformation, with the side chain glycerol/Gal highly exposed. Sugars are colored according to type: blue – Glc/GlcNAc, yellow – Gal, grey – Gro. The O-acetyl substituent is highlighted in red.

In contrast, sera from PCV20-immunized subjects had low titers against both serotype 15A strains (PFE593551 and PFE647449), with GMTs of 10 and 30 (Table 3), indicating very limited or no cross-functional killing antibodies against serotype 15A isolates. The Tdap controls yielded GMTs of 6 against both 15A strains (Table 3).

To confirm the 15C cross-functional human responses, sera from larger sample size in a more relevant age group (60–64-year–old) were used, with one cohort (n = 83) administered

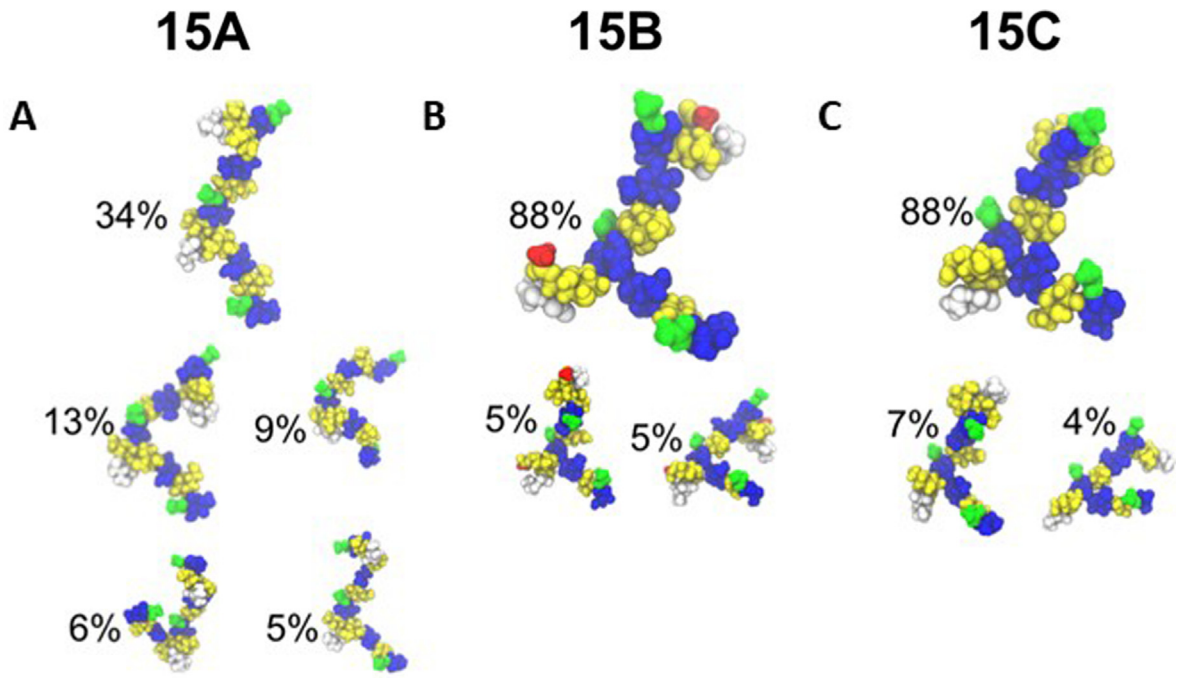

Fig. 4. Conformational families produced by clustering analysis of the simulation of 3RU of (**A**) serotype 15A, (**B**) serotype 15B and (**C**) serotype 15C polysaccharides. Residues are colored according to type: blue – Glc/GlcNAc, yellow – Gal, white – Gro2P (glycerol phosphate). N-Acetyl and O-Acetyl groups are colored green and red, respectively.

Table 3
Serotype 15B, 15C, and 15A cross-functional responses in 18–49-year–old adults. GMT, geometric mean titer; n, number of subjects.

Serotype/Strain	Vaccine group	n	GMT
15B-PFESP05051	Tdap	33	34
	PCV20	32	19,334
15C/PFE344340	Tdap	33	9
	PCV20	32	1692
15C/PFE1160	Tdap	33	12
	PCV20	32	2747
15A/PFE593551	Tdap	33	6
	PCV20	32	10
15A/PFE647449	Tdap	33	6
	PCV20	32	30

PCV20, which contains 15B capsular polysaccharide conjugate, and another (n = 81) administered PCV13, which does not. Analysis of serum immune responses demonstrated the 15C OPA GMT of 164 (95% CI: 94.2, 286.8) for the PCV20 group and GMT of 14 (95% CI: 9.9, 19.2) for the PCV13 group. The 15B OPA GMT for the same PCV20 group was 5107, and for the PCV13 group was 44. Additionally, the 15C GMR between the PCV20 and PCV13 groups was 11.9 (95% CI: 6.25, 22.84), indicating that the 15B–containing PCV20 elicited cross- functional immune responses to 15C. This is also observed via a separation in the 15C OPA antibody titer reverse cumulative distribution curves (RCDCs) for the PCV20 and PCV13 groups (Fig. 6).

4. Discussion

S. pneumoniae serotypes 15A, 15B, and 15C possess highly similar capsular polysaccharide structures that are difficult to distinguish using common serological approaches. The primary differences are a shorter side chain and a longer backbone repeat unit in the 15A polysaccharide compared with 15B and 15C [18], and the presence (15B) or absence (15C) of the *O*-acetyl group on the αDGal in their three-residue side chain in 15B and 15C polysaccharides [17,37]. Differences in the *wzy* polymerase gene between serotypes 15A and 15B/C lead to a linear repeat unit capsular polysaccharide structure in serotype 15A but a branched polysaccharide repeat unit structure in serotypes 15B and 15C [19]. Based on results by Bentley et al. (2006; Fig. 2) [19] comparing the *cps* locus among pneumococcal serotypes, multiple regions of *cps* (including *wzd*, *wchA*, *wzy*, etc.) show differences between serotypes 15A and 15C. Here, the first large segment from 5′ end of the *cps* operon that could be used to differentiate 15A from 15B/C was selected, which does not exclude the possibility that another 15A-specific marker is present in *wzy* or other genes. *O*-acetylation in the 15B polysaccharide is due to activity of *O*-acetyltransferase encoded by the intact gene *cps15bM*, which is defective in 15C (*cps15cM*) [21]. The presence of an extra TA unit in the short tandem TA repeat in the *O*-acetyltransferase gene (9 in 15C versus 8 in 15B) was shown to make the gene defective, resulting in an expression of a truncated inactive enzyme [21]. This mechanism constitutes the genetic basis for reversible switching between the 15B and 15C serotypes that has been reported previously [21,37]. However, no switching has been observed for the 15B production strain used for PCV20 manufacturing (data not shown). Here, a novel genetic method is described that allowed discrimination of serotype 15B and 15C isolates. The implementation of this method will facilitate the ability to accurately identify serotype 15B and 15C isolates and thus improve epidemiologic tracking of isolates causing pneumococcal disease.

Molecular modeling simulations were used in the present report to explore the structure of serogroup 15 polysaccharides. The analyses identified that serotype 15A polysaccharide is a flexible molecule with no well-defined single conformation, while serotype 15B and 15C polysaccharides are constrained to a "zig-zag" conformation, similar to the conformation adopted by pneumococ-

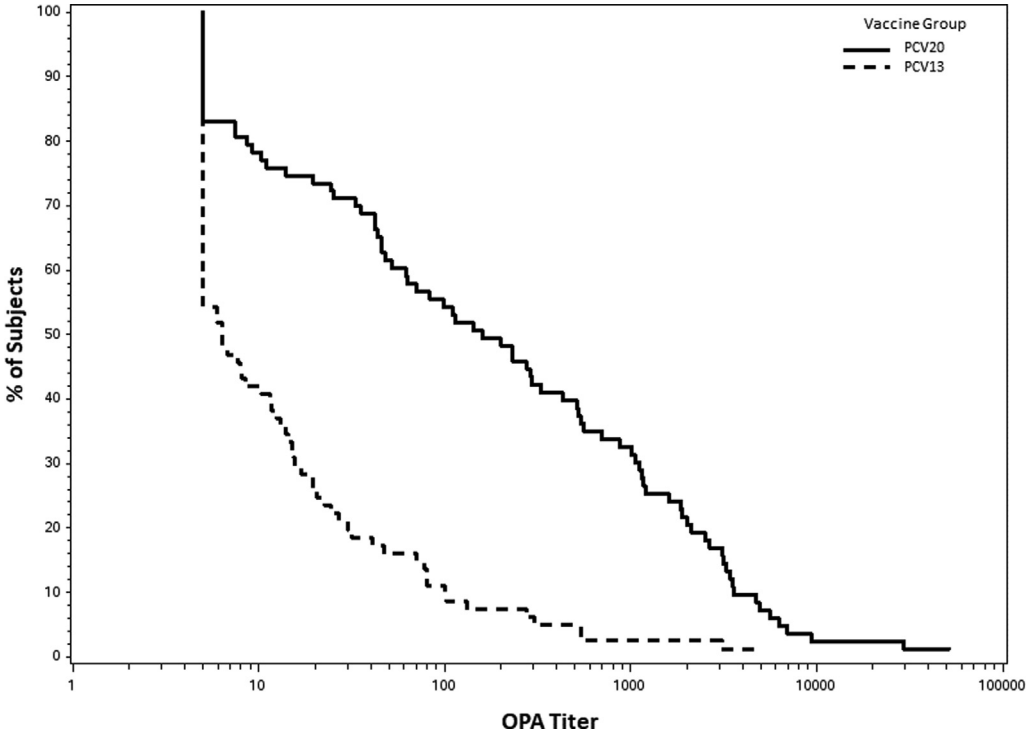

Fig. 6. Serotype 15C OPA antibody titer reverse cumulative distribution curves.

cal serotype 14 or group B streptococcus type III polysaccharides [25]. O-acetylation in 15B is on the end of the branch so it does not disrupt this chain conformation. Given that antibodies can recognize a three-dimensional epitope, a more defined structure, as observed with pneumococcal serotypes 15B and 15C, could present similar epitopes for antibody binding and thus elicit cross-functional antibody responses. In contrast, the random coil of serotype 15A would present a multitude of conformational epitopes to the immune system, and thus could elicit antibodies that are functionally distinct from those recognizing serotypes 15B and 15C.

The ability of 15B capsular polysaccharide conjugate to elicit cross-functional immune responses to 15C but not 15A was confirmed experimentally by demonstrating that subjects immunized with PCV20, a 15B capsular polysaccharide conjugate-containing vaccine, elicited high titers of cross-functional OPA antibodies against 15C strains, but only low responses were observed against 15A. This cross–functional activity was confirmed with a larger serum sample set against a single 15C strain. Together, these data indicate that PCV20 elicits a cross-functional killing immune response to serotype 15C, which is consistent with genetic relatedness and structural similarity between capsular polysaccharides of serotypes 15B and 15C. Although the titers elicited against 15C were lower than against 15B, they were still sizable. This result is consistent with earlier findings on cross-protection: 6B capsular polysaccharide conjugate-containing vaccines can elicit OPA antibody responses to 6A in immunized infants [41,42], and PCV13, which contains capsular polysaccharide conjugates of 6A and 7F, induces cross-functional antibody responses against the related serotypes 6C and 7A, respectively [15]. Of note, although on a sequence level 6A is more similar to 6B, conformationally 6A and 6C are more similar, which could explain why 6A and 6C are more cross-reactive [43].

Following the introduction of PCV13, non-vaccine serotypes 15B and 15C have emerged as prevalent *S. pneumoniae* serotypes in both low- and high-income countries [44–46]. 15B is one of the serotypes currently associated with relatively high case-fatality rates [47–50], meningitis [51,52], and antibiotic resistance [53,54]. PCV20 is expected to provide further protection from pneumococcal disease due to more expanded serotype coverage [55]. Cross-functional antibody responses generated by capsular polysaccharide conjugates included in the vaccine against serotypes with structurally related capsular polysaccharides have the potential to provide additional protection beyond the serotypes directly covered by the vaccine. Although the 15B-conjugate–containing vaccine elicited lower titers against a 15C strain than a 15B strain, the cross-functional responses shown here between serotypes 15B and 15C indicate that the inclusion of 15B conjugate in PCV20 has the potential to provide clinical benefit against serotype 15C. Longitudinal epidemiological trends in pneumococcal disease due to serotype 15C after introduction and uptake of PCV20 will be needed to assess the real-world impact of this cross-functional activity on both invasive disease and nasopharyngeal carriage.

Author contributions

All authors met ICMJE criteria for authorship and participated in the study design (LH, MK, NR, AKP, SG, CT, DC, WW, MP, KUJ, ASA, IS), performing experiments (LH, SG) or computer simulations (MK), data analysis and interpretation (LH, MK, NR, AT, AKP, SG, CT, DC, WW, PL, MP, KUJ, ASA, IS), and manuscript preparation (LH, MK, NR, AT, AKP, SG, CT, DC, WW, PL, MP, KUJ, ASA, IS). All authors approved the final version for journal submission and agree to be accountable for all aspects of the work.

Funding statement

This work was funded by Pfizer Inc.

Declaration of Competing Interest

The authors declare the following financial interests/personal relationships which may be considered as potential competing interests: [Ingrid Scully, Li Hao, Allison Thompson, Seema Gangolli, Charles Tan, David Cooper, Wendy Watson, Paul Liberator, Michael Pride, Kathrin Jansen and Annaliesa Anderson are all employees of Pfizer and as such may hold stock and stock options. A. Krishna Prasad was an employee of Pfizer at the time the work was conducted but has since left the company. Michelle M. Kuttel reports a relationship with Pfizer Inc that includes: funding grants. Neil Ravenscroft reports a relationship with Pfizer Inc that includes: funding grants.].

Acknowledgements

The authors thank the following Pfizer Inc. Vaccine Research and Development colleagues: Jonathan Lee for the development of a WGS-based serotyping tool and implementation of this tool on serogroup 15 isolates, Yahong Peng for critical review and statistical input, Robert Donald for critical review, and the Clinical and Diagnostic Assay Development team for performing serotype-specific OPA assays. Computations were performed using facilities provided by the University of Cape Town's ICTS High Performance Computing team (http:// hpc.uct.ac.za). The authors thank Nataliya Kushnir, Pfizer Inc. for scientific writing assistance.

Appendix A. Supplementary material

Supplementary data to this article can be found online at https://doi.org/10.1016/j.vaccine.2022.06.041.

References

[1] Feldman C, Anderson R. Epidemiology, virulence factors and management of the pneumococcus. F1000Res 2016;5:2320.
[2] Pilishvili T, Lexau C, Farley M, Hadler J, Harrison L, Bennett N, et al. Sustained reductions in invasive pneumococcal disease in the era of conjugate vaccine. J Infect Dis 2010;201(1):32–41.
[3] Robinson KA, Baughman W, Rothrock G, Barrett NL, Pass M, Lexau C, et al. Epidemiology of invasive Streptococcus pneumoniae infections in the United States, 1995–1998: Opportunities for prevention in the conjugate vaccine era. JAMA 2001;285:1729–35.
[4] Wahl B, O'Brien KL, Greenbaum A, Majumder A, Liu Li, Chu Y, et al. Burden of Streptococcus pneumoniae and Haemophilus influenzae type b disease in children in the era of conjugate vaccines: global, regional, and national estimates for 2000–15. Lancet Glob Health 2018;6(7):e744–57.
[5] Briles DE, Crain MJ, Gray BM, Forman C, Yother J. Strong association between capsular type and virulence for mice among human isolates of Streptococcus pneumoniae. Infect Immun 1992;60(1):111–6.
[6] Daniels CC, Rogers PD, Shelton CM. A Review of Pneumococcal Vaccines: Current Polysaccharide Vaccine Recommendations and Future Protein Antigens. J Pediatr Pharmacol Ther 2016;21:27–35.
[7] Geno KA, Gilbert GL, Song JY, Skovsted IC, Klugman KP, Jones C, et al. Pneumococcal Capsules and Their Types: Past, Present, and Future. Clin Microbiol Rev 2015;28(3):871–99.
[8] Kamerling JP. Pneumococcal polysaccharides: a chemical view. In: (ed.) IAT, editor. Streptococcus pneumoniae: molecular biology and mechanisms of disease. Larchmont, N.Y.: Mary Ann Liebert, Inc.; 1999. p. 81-114.
[9] van Tonder AJ, Gladstone RA, Lo SW, Nahm MH, du Plessis M, Cornick J, et al. Putative novel cps loci in a large global collection of pneumococci. Microb Genom 2019;5(7):e000274.
[10] Hu BT, Yu X, Jones TR, Kirch C, Harris S, Hildreth SW, et al. Approach to validating an opsonophagocytic assay for Streptococcus pneumoniae. Clin Diagn Lab Immunol 2005;12:287–95.
[11] Lortan JE, Kaniuk AS, Monteil MA. Relationship of in vitro phagocytosis of serotype 14 Streptococcus pneumoniae to specific class and IgG subclass antibody levels in healthy adults. Clin Exp Immunol 1993;91:54–7.
[12] Romero-Steiner S, Libutti D, Pais LB, Dykes J, Anderson P, Whitin JC, et al. Standardization of an opsonophagocytic assay for the measurement of

functional antibody activity against Streptococcus pneumoniae using differentiated HL-60 cells. Clin Diagn Lab Immunol 1997;4(4):415–22.
[13] Soininen A, Karpala M, Wahlman S-L, Lehtonen H, Käyhty H. Specificities and opsonophagocytic activities of antibodies to pneumococcal capsular polysaccharides in sera of unimmunized young children. Clin Diagn Lab Immunol 2002;9(5):1032–8.
[14] Winkelstein JA. The role of complement in the host's defense against Streptococcus pneumoniae. Rev Infect Dis 1981;3(2):289–98.
[15] Cooper D, Yu X, Sidhu M, Nahm MH, Fernsten P, Jansen KU. The 13-valent pneumococcal conjugate vaccine (PCV13) elicits cross-functional opsonophagocytic killing responses in humans to Streptococcus pneumoniae serotypes 6C and 7A. Vaccine 2011;29(41):7207–11.
[16] Pfizer. PREVNAR 20 (Pneumococcal 20-valent Conjugate Vaccine). Prescribing Information. https://www.fda.gov/media/149987/download. Accessed 13 June, 2021. 2021.
[17] Jansson P-E, Lindberg B, Lindquist U, Ljungberg J. Structural studies of the capsular polysaccharide from Streptococcus pneumoniae types 15B and 15C. Carbohydr Res 1987;162(1):111–6.
[18] Kolkman MAB, van der Zeijst BAM, Nuijten PJM. Diversity of capsular polysaccharide synthesis gene clusters in Streptococcus pneumoniae. J Biochem 1998;123(5):937–45.
[19] Bentley SD, Aanensen DM, Mavroidi A, Saunders D, Rabbinowitsch E, Collins M, et al. Genetic analysis of the capsular biosynthetic locus from all 90 pneumococcal serotypes. PLoS Genet 2006;2(3):e31.
[20] Kapatai G, Sheppard CL, Al-Shahib A, Litt DJ, Underwood AP, Harrison TG, et al. Whole genome sequencing of Streptococcus pneumoniae: development, evaluation and verification of targets for serogroup and serotype prediction using an automated pipeline. PeerJ 2016;4:e2477.
[21] van Selm S, van Cann LM, Kolkman MAB, van der Zeijst BAM, van Putten JPM. Genetic basis for the structural difference between Streptococcus pneumoniae serotype 15B and 15C capsular polysaccharides. Infect Immun 2003;71(11):6192–8.
[22] Andam CP, Mitchell PK, Callendrello A, Chang Q, Corander J, Chaguza C, et al. Genomic Epidemiology of Penicillin-Nonsusceptible Pneumococci with Nonvaccine Serotypes Causing Invasive Disease in the United States. J Clin Microbiol 2017;55(4):1104–15.
[23] Gladstone RA, Devine V, Jones J, Cleary D, Jefferies JM, Bentley SD, et al. Pre-vaccine serotype composition within a lineage signposts its serotype replacement - a carriage study over 7 years following pneumococcal conjugate vaccine use in the UK. Microb Genom 2017;3(6):e000119.
[24] Laufer AS, Thomas JC, Figueira M, Gent JF, Pelton SI, Pettigrew MM. Capacity of serotype 19A and 15B/C Streptococcus pneumoniae isolates for experimental otitis media: Implications for the conjugate vaccine. Vaccine 2010;28(12):2450–7.
[25] Kuttel MM, Ravenscroft N. Conformation and Cross-Protection in Group B Streptococcus Serotype III and Streptococcus pneumoniae Serotype 14: A Molecular Modeling Study. Pharmaceuticals (Basel) 2019;12:28.
[26] Phillips JC, Braun R, Wang W, Gumbart J, Tajkhorshid E, Villa E, et al. Scalable molecular dynamics with NAMD. J Comput Chem 2005;26(16):1781–802.
[27] Stone JE, Phillips JC, Freddolino PL, Hardy DJ, Trabuco LG, Schulten K. Accelerating molecular modeling applications with graphics processors. J Comput Chem 2007;28(16):2618–40.
[28] Guvench O, Greene SN, Kamath G, Brady JW, Venable RM, Pastor RW, et al. Additive empirical force field for hexopyranose monosaccharides. J Comput Chem 2008;29(15):2543–64.
[29] Guvench O, Hatcher E, Venable RM, Pastor RW, MacKerell AD. CHARMM additive all-atom force field for glycosidic linkages between hexopyranoses. J Chem Theory Comput 2009;5(9):2353–70.
[30] Jorgensen WL, Chandrasekhar J, Madura JD, Impey RW, Klein ML. Comparison of simple potential functions for simulating liquid water. J Chem Phys 1983;79(2):926–35.
[31] Kuttel MM, Ståhle J, Widmalm G. CarbBuilder: Software for building molecular models of complex oligo- and polysaccharide structures. J Comput Chem 2016;37(22):2098–105.
[32] Humphrey W, Dalke A, Schulten K. VMD: visual molecular dynamics. J Mol Graph 1996;14(33–8):27–8.
[33] Martyna GJ, Tobias DJ, Klein ML. Constant pressure molecular dynamics algorithms. J Chem Phys 1994;101(5):4177–89.
[34] Feller SE, Zhang Y, Pastor RW, Brooks BR. Constant pressure molecular dynamics simulation: the Langevin piston method. J Chem Phys 1995;103(11):4613–21.
[35] Darden T, York D, Pedersen L. Particle mesh Ewald: An N· log (N) method for Ewald sums in large systems. J Chem Phys 1993;98(12):10089–92.
[36] Gray BM. Opsonophagocidal activity in sera from infants and children immunized with Haemophilus influenzae type b conjugate vaccine (meningococcal protein conjugate). Pediatrics 1990;85:694–7.
[37] Venkateswaran PS, Stanton N, Austrian R. Type variation of strains of Streptococcus pneumoniae in capsular serogroup 15. J Infect Dis 1983;147(6):1041–54.
[38] Jolley KA, Maiden MC. BIGSdb: Scalable analysis of bacterial genome variation at the population level. BMC Bioinf 2010;11:595.
[39] Reasonover A, Zulz T, Bruce MG, Bruden D, Jetté L, Kaltoft M, et al. The International Circumpolar Surveillance interlaboratory quality control program for Streptococcus pneumoniae, 1999 to 2008. J Clin Microbiol 2011;49(1):138–43.
[40] Slotved H-C, Sheppard CL, Dalby T, van der Ende A, Fry NK, Morfeldt E, et al. External quality assurance for laboratory identification and capsular typing of streptococcus pneumoniae. Sci Rep 2017;7(1).
[41] Väkeväinen M, Eklund C, Eskola J, Käyhty H. Cross-reactivity of antibodies to type 6B and 6A polysaccharides of Streptococcus pneumoniae, evoked by pneumococcal conjugate vaccines, in infants. J Infect Dis 2001;184(6):789–93.
[42] Yu X, Gray B, Chang S-j, Ward J, Edwards K, Nahm M. Immunity to cross-reactive serotypes induced by pneumococcal conjugate vaccines in infants. J Infect Dis 1999;180(5):1569–76.
[43] Kuttel MM, Ravenscroft N. The Role of Molecular Modeling in Predicting Carbohydrate Antigen Conformation and Understanding Vaccine Immunogenicity. In: Prasad AK, editor. Carbohydrate-Based Vaccines: From Concept to Clinic: American Chemical Society; 2018. p. 139-73.
[44] Croucher NJ, Finkelstein JA, Pelton SI, Mitchell PK, Lee GM, Parkhill J, et al. Population genomics of post-vaccine changes in pneumococcal epidemiology. Nat Genet 2013;45(6):656–63.
[45] Gladstone RA, Jefferies JM, Tocheva AS, Beard KR, Garley D, Chong WW, et al. Five winters of pneumococcal serotype replacement in UK carriage following PCV introduction. Vaccine 2015;33(17):2015–21.
[46] Ho P-L, Chiu SS, Law PY, Chan EL, Lai EL, Chow K-H. Increase in the nasopharyngeal carriage of non-vaccine serogroup 15 Streptococcus pneumoniae after introduction of children pneumococcal conjugate vaccination in Hong Kong. Diagn Microbiol Infect Dis 2015;81(2):145–8.
[47] Harboe ZB, Thomsen RW, Riis A, Valentiner-Branth P, Christensen JJ, Lambertsen L, et al. Pneumococcal serotypes and mortality following invasive pneumococcal disease: a population-based cohort study. PLoS Med 2009;6(5):e1000081.
[48] Oligbu G, Collins S, Sheppard CL, Fry NK, Slack M, Borrow R, et al. Childhood deaths attributable to invasive pneumococcal disease in England and Wales, 2006–2014. Clin Infect Dis 2017;65(2):308–14.
[49] Stanek RJ, Norton NB, Mufson MA. A 32-year study of the effect of pneumococcal vaccines on invasive streptococcus pneumoniae disease. Am J Med Sci 2016;352(6):563–73.
[50] van Hoek AJ, Andrews N, Waight PA, George R, Miller E, Aguilar L. Effect of serotype on focus and mortality of invasive pneumococcal disease: coverage of different vaccines and insight into non-vaccine serotypes. PLoS ONE 2012;7(7):e39150.
[51] Olarte L, Barson WJ, Barson RM, Lin PL, Romero JR, Tan TQ, et al. Impact of the 13-valent pneumococcal conjugate vaccine on pneumococcal meningitis in US children. Clin Infect Dis 2015;61(5):767–75.
[52] Thigpen MC, Whitney CG, Messonnier NE, Zell ER, Lynfield R, Hadler JL, et al. Bacterial meningitis in the United States, 1998–2007. N Engl J Med 2011;364(21):2016–25.
[53] Metcalf BJ, Gertz RE, Gladstone RA, Walker H, Sherwood LK, Jackson D, et al. Strain features and distributions in pneumococci from children with invasive disease before and after 13-valent conjugate vaccine implementation in the USA. Clin Microbiol Infect 2016;22(1):60.e9–60.e29.
[54] Tomczyk S, Lynfield R, Schaffner W, Reingold A, Miller L, Petit S, et al. Prevention of antibiotic-nonsusceptible invasive pneumococcal disease with the 13-valent pneumococcal conjugate vaccine. Clin Infect Dis 2016;62(9):1119–25.
[55] Thompson A, Lamberth E, Severs J, Scully I, Tarabar S, Ginis J, et al. Phase 1 trial of a 20-valent pneumococcal conjugate vaccine in healthy adults. Vaccine 2019;37(42):6201–7.